2011

Solving evolution equations for triad interaction of shallow water waves

Qian Zhang
Louisiana State University and Agricultural and Mechanical College

SOLVING EVOLUTION EQUATIONS FOR TRIAD INTERACTION OF SHALLOW WATER WAVES

A Thesis

Submitted to the Graduate Faculty of the
Louisiana State University and
Agricultural and Mechanical College
in partial fulfillment of the
requirements for the degree of
Master of Science in Engineering Science

in

The Interdisciplinary Departmental Program in Engineering Science

By
Qian Zhang
B.S., Harbin Engineering University, 2006
M.S., Harbin Institute of Technology, 2008

August 2011

ACKNOWLEDGEMENTS

First of all, I would like to express my deep gratitude to my advisor Dr. Q. Jim Chen, who made this research possible and indoctrinates me in the research process. His support, guidance, patience and faith through every bump in the road were invaluable. Thanks also to my committee members Dr. Frank Tsai and Dr. Xiaoliang Wan for their sincere help and professional advice on the thesis.

I would also like to thank Dr. Haihong Zhao, Dr. Jian Tao and Dr. Kelin Hu who have shared their experience in numerical modeling and thesis writing. I want furthermore to acknowledge the assistance I received from my fellow students Qi Fan, Ling Zhu, Ke Liu, and Agnimitro Chakrabarti for their encouragement and valuable suggestions.

Finally, I would like to give my special thanks to my parents and friends for their unconditional love and support. Thanks for being there for me through all of the ups and downs.

Table of Contents

LIST OF TABLES

LIST OF FIGURES

ABSTRACT

This study focuses on solving the evolution equations for triad interaction in shallow water waves. First, the evolution equations based on Boussinesq-type equations with Padé approximant of the exact linear phase velocity using multi-scale perturbation analysis are derived. Next, methods of solving the complex equation directly, splitting the complex function into amplitude and phase functions, and splitting complex function into real and imaginary parts are implemented to solve the evolution equations. Then the fourth-order Runge-Kutta (RK4) numerical scheme is employed to solve the evolution equations, and corresponding numerical results of three wave interaction are presented demonstrating the sensitivity of the model to the perturbation parameter ε. When ε=0.45, the model produces the optimal result in good agreement with the exact solution in terms of beat length as well as amplitude. The method of manufactured solutions (MMS) is utilized to verify the codes, ensuring that they have been coded correctly and are fulfilled with the capability to solve the equations.

CHAPTER 1 INTRODUCTION

1.1 Background

In shallow water, the phenomenon that a simple sinusoidal wave generates higher harmonic waves during propagation has been observed (e.g., Goda, 1967, Freilich and Guza,1984). The concept of near resonance (Armstrong et al., 1962, Bretherton, 1964) was used to show wave energy exchange due to nonlinear interactions among those harmonics. The strength of the interaction is governed by the phase mismatch between bound and free wave numbers, and the so-called beat length is the distance between two successive recurrences (energy cycling among wave frequencies, Kaihatu (2009)), where energy transfers back and forth in short distances. This results in a spatial variation of wave profiles and spectral parameters.

Waves that are considered to be in shallow water are located within a water depth to the wave length ratio of less than 0.05. Common wave transformations occurring in intermediate and shallow water (the water depth is less than half of the wave length.) include wave shoaling, refraction, reflection, diffraction and breaking. When waves propagate from deep to shallow water, they slow down, grow taller and change shape. This transformation is descried as wave shoaling in coastal zone processes. The wave shoals when the wave is approaching a shoreline perpendicular with the wave length shortened. If waves come closer to the shore at an angle, wave refraction takes place because of varying water depth. Wave refraction on a planar beach can be described by the Snell's law, which relates the wave angle variation with the wave celerity change. According to the Snell's law, the wave angle decreases as the wave slows down from

deep to shallow water, and the wave crest begins to bend parallel to the shoreline. Throughout wave shoaling and refraction processes, the wave period remains the same and the wave energy flux is conserved. When waves encounter a surface piercing obstacle, the wave energy might be partially or completely reflected in the opposite direction to the incident wave direction. This phenomenon is defined as wave reflection and the percentage of reflection is usually dependent on properties such as shape and construction material of the obstruction. Wave energy transfer laterally along the wave crest may also happen in the case of obstacles, this process is known as wave diffraction. An example of diffraction would be when waves pass an obstacle that creates a sheltered zone behind it and the waves diffract into this zone. It is also worth mentioning that wave diffraction and refraction occur at the same time but the mechanisms of both are completely different. When the wave crest becomes too steep during shoaling, it becomes unstable, curls forward and finally breaks. Wave breaking is a process through which a wave dissipates its energy. Wave breaking also leads to the generation of surf zone currents. The usual breaking criterion in shallow water is a wave height that exceeds 0.78 of the local water depth. After the wave breaks, it becomes a wave of translation that intensifies erosion of the ocean bottom, and triggers sediment transport.

Among all these coastal processes in shallow water, it is the nonlinear effect that is responsible for the changes in wave shape and produces a number of harmonic components of the frequency spectrum from the original wave. As a wave propagates, it will also dissipate some energy due to interaction at the air-water surface and in shallower water at the sea-bed interface. The focus of this study lies in the wave energy transfer between waves.

1.2 Boussinesq Wave Theory

Regular waves are also called monochromatic waves, defined as waves with the same wave period, wave height, and direction. And sinusoidal waves are the simplest form of regular waves. Wave theories for regular waves can be broken into linear wave theory (Airy theory or small amplitude theory) and nonlinear wave theory. Boussinesq wave theory is one of the nonlinear theories in shallow water.

Since Boussinesq (1871) proposed the Boussinesq equations in one-dimension of a constant depth, it has played a very important role in the study of nonlinear waves in shallow water. For over a century, the Boussinesq theory has been extended to short waves in deeper water and has become a powerful tool to simulate wave propagation in coastal regions. Among those efforts, Peregrine (1967) proposed the classical Boussinesq equations for waves in shallow water with varying depth in two dimensions. Then, Witting (1984) gave a more accurate unified wave model for both shallow and deep water waves but this model was still limited to one dimensional constant depth. Padé-type expansion of the dispersion relation obtained by Madsen et al. (1991), Madsen and Sørensen (1993), Nwogu (1993), Schröer et al. (1994), Schäffer and Madsen (1995) and others advanced the dispersion properties of the Boussinesq equations for wave propagation in intermediate and deep water. Kristensen (1995) made an attempt to extend the Boussinesq theory for wave/current interaction for larger wave numbers. Mei and Ünlüata (1972), Freilich and Guza (1984), Madsen and Sørensen (1993), successfully applied the classical and extended Boussinesq equations to study nonlinear triad interaction of water waves. Also, Mei (1989), Dingemans (1997) and Chen et al. (1999)

derived the evolution equations for triad interaction in shallow water based on Boussinesq-type equations.

1.3 Harmonic Generation and Nonlinear Interactions on a Constant Depth

Harmonic generation is one of the simplest examples of nonlinear interactions which occur when first order boundary conditions (equal amplitude and opposite phase compared to bound waves) are applied in shallow water. This well-known phenomenon has been studied experimentally by, for example, Boczar-Karakiewicz (1972), Buhr-Hansen and Svendsen (1974), and Chapalain et al. (1992), and theoretically by Mei and Ünlüata (1972), Bryant (1973), Mei (1983), and Madsen and Sørensen (1993) among others. In the laboratory, if we put a sinusoidal wave at the boundary, we will never be able to generate a nice sinusoidal wave in the wave flume especially when the water depth is small and the wave height is large. As regular waves propagate in shallow water, they will decompose into free first harmonics and bound higher harmonics. The first-order inflow boundary condition plays a role in excluding the generation of bound higher harmonics and therefore leading to release of parasitic higher harmonics which are of equal amplitude and opposite phase compared to bound waves and propagate as free wave components. The superposition of the free and bound spurious waves leads to the spatially varying amplitude and serves as the principle of harmonic generation. Generally the free parasitic second harmonic will interact with the primary wave to generate sum and difference frequencies. The sub-harmonic interaction of ω_1 and $2\omega_1$ leads to the change of energy at frequency ω_1 with the governing phase mismatch being $\delta^- = k_2 - 2k_1$; while the super-harmonic interaction between ω_1 and $2\omega_1$ leads to the generation of a third harmonic $3\omega_1$ with the governing phase mismatch $\delta^+ = k_3 - k_2 - k_1$ (Madsen

and Sørensen, 1993, Chen et al., 1999). In order to accurately describe the phenomena of harmonic generation and nonlinear interactions, evolution equations are required.

1.4 Objectives

The physical process of triad interaction exchanges wave energy among three harmonics and generally occurs in shallow and intermediate water. The objectives of this thesis are

1). to solve the evolution equations for triad interaction of shallow water waves by three different methods, then compare the numerical results with the exact solution solving the fully nonlinear Boussinesq equations by a finite difference scheme in Chen et al. (1999) ,

2). to test the numerical solutions to the evolution equations using the method of manufactured solutions (MMS), and

3). to obtain a better understanding of the effect of the perturbation parameter on the accuracy of the evolution equations by carrying out a series of numerical experiments with a range of values for the perturbation parameter.

1.5 Overview of Thesis

The thesis is organized as follows: Chapter 1 introduces the phenomenon of nonlinear triad interaction and provides a foundation for the theoretical background. A review of the available literature on topics of harmonic generation is provided in Chapter 2. Based on the research published in the literature, the problem to be solved in this thesis is defined and posed. Chapter 3 details the numerical methods, including characteristics of different approaches as well as the methodology to verify the numerical results using the method of manufactured solutions (MMS). Chapter 4 presents and discusses the

numerical results obtained, their comparison with the exact solutions, and the significance of these results. Finally, Chapter 5 summarizes the modeled results and brings up some recommendations for future work related to the study.

CHAPTER 2 LITERATURE REVIEW AND PROBLEM STATEMENT

As discussed in Chapter 1, the overall aims of this study are to solve the evolution equations of triad interaction and to examine the simulated wave energy exchange in shallow water. Therefore, it is necessary to discuss the literature written on this subject. This chapter initially discusses the discoveries of wave-wave interaction and then moves on to wave-current interaction as well as various mathematical formulations that have been derived to describe these processes. The final section of this chapter then states the problem to be studied in this thesis.

2.1 Literature Review

Since the 1960s, experiments on progressive shallow water waves in wave tanks have shown a new secondary crest between two successive crests (Goda, 1967, Galvin, 1968), and this harmonic generation has captured the attention of physical oceanographers and coastal engineers. In the beginning, the classical Boussinesq equations were used to study triad interaction of periodic waves in shallow water by Mei and Ünlüata (1972), Bryant (1973), and Dingemans (1997). However, Madsen and Sørensen (1993) considered bound waves and triad interaction on a horizontal and mildly sloping bottom in a numerical wave flume based on improved Boussinesq-type equations, eliminating the accuracy limitation of higher harmonics generated by the classical Boussinesq models. Numerical results by time domain finite difference models and by frequency domain models based on derived evolution equations with b=1/15 and Fourier series approximation to the Boussinesq equations were proved to agree well with experimental data, in terms of beat length and the maximum amplitude of the second

harmonic. Dingemans (1997) investigated the phenomenon of nonlinear generation of higher- and lower-harmonic wave components based on Boussinesq-type equations and derived the evolution equations for pure three-wave motion through the multi-scale perturbation approach. The analysis involving more than three harmonics was given by, for example, Bryant (1973, 1983), Freilich and Guza (1984), Kirby (1991), Madsen and Sørensen (1993) and Won and Battjes (1992). Bryant (1973) also worked on the three-wave interaction based on the KdV equation. The more general problem of nonlinear shoaling of irregular wave trains was treated by Freilich and Guza (1984), and Madsen and Sørensen (1993), among others.

Wave dynamics in coastal regions can be strongly affected by the presence of currents. It is therefore necessary and important to understand the current effects on nonlinear wave interaction. Wave-current interaction in shallow water was first studied by Yoon and Liu (1989) on the basis of the classical Boussinesq equations. Prüser and Zielke (1990) investigated the wave interaction with large scale currents, such as tidal currents. Similar to the performance of the classical Boussinesq equations, the sets of equations are limited to relatively small wave numbers. Elgar et al. (1990) stated that recurrence in many-mode systems such as random waves without currents is not a prevalent feature. However, Chen et al. (1999) showed by three modes that the degree of recurrence is enhanced by following currents and reduced by adverse currents. Chen et al. (1999) also derived the evolution equations based on Yoon and Liu's (1989) equations that govern the energy transfer between frequencies. They also showed that the energy exchange between the primary wave and higher harmonics was increased by the following current but decreased by the adverse current, which has been confirmed by

Kaihatu's (2009) work. Kaihatu (2009) used the frequency domain nonlinear wave-current interaction model to investigate the phenomenon of wave recurrence in random wave evolution over a flat bottom, including a second-order correction similar to that of Kaihatu (2001) to improve the model's accuracy. He showed that for moderate Ursell numbers, the recurrence follows the feature of monochromatic waves in a very limited distance and afterwards is completed damped. However for high Ursell numbers, the recurrence is immediately damped regardless of the current magnitude and direction. Chen et al. (1998) and Madsen and Schäffer (1998) solved Boussinesq-type equations in the time domain using a higher-order finite difference method for wave blocking by strong currents and current effects on harmonic generation and nonlinear interactions of shallow water waves.

2.2 Problem Statement

Although Chen et al. (1999) derived the evolution equations for triad interaction based on Yoon and Liu's (1989) equations with a constant depth and an ambient current to provide insight into the complicated water wave phenomenon, the numerical experiments on harmonic generation and nonlinear energy transfer were not based on the derived evolution equations but on the enhanced Boussinesq-type model by Madsen and Schäffer (1998) with higher dispersion accuracy for wave/current interaction. Even though Dingemans (1997) also investigated triad interaction based on the evolution equations derived from Boussinesq-type equations, discussed the exact solution for two-wave interaction case, and showed the numerical results for three wave interactions, to my knowledge, we have not seen any analysis on the accuracy of the evolution equations. If the evolution equations are not accurate enough, is there any factor that affects the

accuracy of the evolution equations? So the goal of this study is to directly solve the evolution equations in order to investigate the accuracy of the evolution equations for three-wave interaction in comparison with the numerical results of Chen et al. (1999).

The general theoretical descriptions of triad interaction are based on the use of truncated Fourier series. For example, Madsen and Sørensen (1993) considered slowly varying amplitudes and derived the evolution equations for the spatial variation of three amplitudes based on various forms of the Boussinesq and KdV equations. In this study, we follow Dingemans (1997) and Chen et al. (1999) to derive the evolution equations on the basis of Boussinesq-type equations with constant water depth using the multi-scale method, which is simple in spite of less accuracy than Fourier approximation. For better dispersion accuracy, the Boussinesq-type equations based on the Padé approximant of the exact linear phase velocity, derived by Madsen, Murray, and Sørensen (1991), are chosen as the starting point of our analysis.

The one-dimensional version of the model equations on a horizontal bed in dimensional form are given by

$$\frac{\partial \eta}{\partial t} + \frac{\partial}{\partial x}[(h+\eta)u] = 0$$
$$\frac{\partial u}{\partial t} + u\frac{\partial u}{\partial x} + g\frac{\partial \eta}{\partial x} = \left(\frac{1}{3} + b\right)h^2\frac{\partial^3 u}{\partial t\,\partial x^2} + bgh^2\frac{\partial^3 \eta}{\partial x^3} \qquad (2.1)$$

where u denotes the depth-averaged velocity in the x-direction; η is the free surface elevation; and the value b=1/15 comes from the Padé approximant. We assume that the waveform modulation resulting from nonlinear triad interactions is much slower than the spatial variation of the free surface. So after multi-scale expansion, we get the expressions similar to those in Chen et al. (1999):

$$X = \varepsilon x \tag{2.2}$$

$$u = u(x, X, t);\ \eta = \eta(x, X, t) \tag{2.3}$$

$$\eta = \sum_{j=1}^{3} a_j(X) e^{i\emptyset_j} + * \tag{2.4}$$

$$u = \sum_{j=1}^{3} \left(\frac{\omega_j}{k_j h}\right) a_j(X) e^{i\emptyset_j} + * \tag{2.5}$$

where X denotes the slow scale and ε the perturbation parameter set freely or chosen to be the nonlinear parameter, ε=a/h ratio of wave amplitude (a) to still water depth (h); and a_j is the wave amplitude; k_j is the wave number; $*$ denotes the complex conjugate of the foregoing terms; and $\emptyset_j = k_j x - \omega_j t = k_j \frac{X}{\varepsilon} - \omega_j t$, in which the absolute angular frequency is given by $\omega_j = j\omega$; the corresponding dispersion relationship can be obtained

$$\omega_j^2 \left[1 + \left(\frac{1}{3} + b\right)\left(k_j h\right)^2\right] - k_j^2 gh \left[1 + b\left(k_j h\right)^2\right] = 0 \tag{2.6}$$

Solving Equation (2.6) leads to the wave number

$$k_j = \sqrt{\frac{\left(\frac{1}{3}+b\right)(\omega_j h)^2 - gh + \sqrt{\left[\left(\frac{1}{3}+b\right)(\omega_j h)^2 - gh\right]^2 + 4bgh^3\omega_j^2}}{2bgh^3}} \tag{2.7}$$

Inserting Equations (2.4) and (2.5) into (2.1) leads to

$$\begin{cases} \dfrac{da_1}{dX} = -i\dfrac{Q_1}{P_1} a_1^* a_2 e^{i(\emptyset_2 - 2\emptyset_1)} - i\dfrac{R_1}{P_1} a_2^* a_3 e^{i(\emptyset_3 - \emptyset_2 - \emptyset_1)} \\ \dfrac{da_2}{dX} = -i\dfrac{Q_2}{P_2} a_1^2 e^{i(2\emptyset_1 - \emptyset_2)} - i\dfrac{R_2}{P_2} a_1^* a_3 e^{i(\emptyset_3 - \emptyset_2 - \emptyset_1)} \\ \dfrac{da_3}{dX} = -i\dfrac{R_3}{P_3} a_1 a_2 e^{i(\emptyset_1 + \emptyset_2 - \emptyset_3)} \end{cases} \tag{2.8}$$

where

$$P_j = 2g\omega_j[1 - \left(\frac{1}{3} + b\right)\frac{h}{g}\omega_j^2 + \frac{3b(k_j h)^2}{2}] \tag{2.9a}$$

$$Q_1 = \frac{g}{h}(k_2 - k_1)^2\left(\frac{\omega_1}{k_1} + \frac{\omega_2}{k_2}\right) + \frac{1}{h^2}\omega_1\omega_2\left(\frac{1}{k_1} - \frac{1}{k_2}\right)(\omega_2 - \omega_1) \tag{2.9b}$$

$$R_1 = \frac{g}{h}(k_3 - k_2)^2\left(\frac{\omega_2}{k_2} + \frac{\omega_3}{k_3}\right) + \frac{1}{h^2}\omega_2\omega_3\left(\frac{1}{k_2} - \frac{1}{k_3}\right)(\omega_3 - \omega_2) \tag{2.9}$$

$$Q_2 = \frac{4g}{h}\omega_1 k_1 + \frac{2}{h^2}\omega_1^3 \tag{2.9d}$$

$$R_2 = \frac{g}{h}(k_3 - k_1)^2\left(\frac{\omega_1}{k_1} + \frac{\omega_3}{k_3}\right) + \frac{1}{h^2}\omega_1\omega_3\left(\frac{1}{k_1} - \frac{1}{k_3}\right)(\omega_3 - \omega_1) \tag{2.9e}$$

$$R_3 = \frac{g}{h}(k_1 + k_2)^2\left(\frac{\omega_1}{k_1} + \frac{\omega_2}{k_2}\right) + \frac{1}{h^2}\omega_1\omega_2\left(\frac{1}{k_1} + \frac{1}{k_2}\right)(\omega_1 + \omega_2) \tag{2.9f}$$

$$T_j = \frac{Q_j}{P_j}, j = 1,2 \tag{2.9g}$$

$$S_j = \frac{R_j}{P_j}, j = 1,2,3 \tag{2.9h}$$

$$\Delta k = \frac{k_2 - 2k_1}{\varepsilon} \tag{2.9i}$$

$$\delta k = \frac{k_3 - k_2 - k_1}{\varepsilon} \tag{2.9j}$$

The aim of this thesis is to solve the evolution equations (2.8) by different methods. It is obvious that when b=0, the dispersion relationship, the evolution equations with all the coefficients are simplified to the case in Chen et al. (1999).

CHAPTER 3 METHODS

Although the evolution equations are presented in Chapter 2, it is necessary to describe the theoretical technique that transforms the Boussinesq-type governing equations into the evolution equations in terms of slow spatial scale. During this process, the multi-scale perturbation method plays a significant role. In order to solve the evolution equations with complex functions, a further decomposition of the evolution equations derived in Chapter 2 is considered before implementing the numerical scheme. After that, a numerical model is developed to solve the evolution equations and the method of manufactured solutions (MMS) is applied to verify the correctness and effectiveness of the code.

3.1 Multi-scale Perturbation Analysis

Many computational problems faced today by engineers, physicists, and applied mathematicians consist of complex models, nonlinear governing equations, variable coefficients and nonlinear known or unknown boundary conditions, which makes it a difficult task to obtain their exact solutions analytically. One may apply the method of perturbations (asymptotic expansions) in terms of a small or a large parameter or coordinate to solve a nonlinear problem approximately. The theory of perturbation analysis began in 1926 with the papers of Rayleigh (1927) and Schrödinger (1926), who treated eigenvalues and applications in acoustic physics. They were also the first papers from a mathematical point of view, formal but incomplete. Rellich (1936) was the first one to consider the convergence of expansion series of perturbation theory. Nayfeh (1978) introduced various perturbation methods in a systematic and comprehensive way.

The principle of perturbation theory is to represent the desired solution in terms of power series in some small parameter that quantifies the deviation from the exact solvable problem. Different from Taylor series where the coefficient is determined by the order of derivative of the function at a specific point, the leading term in perturbation power expansion is the known solution to the exact solvable problem and further terms represent the high-order terms, describing the deviation from the initial problem. For a small perturbation parameter, these high-order terms in the series become successively smaller. Thus an approximated perturbation solution is obtained by truncating the series, usually by keeping only the first several terms, including the initial condition and the first-order perturbation correction.

In this study, it is the slower waveform modulation resulting from nonlinear interactions of three harmonics rather than the spatial variation of the free surface that we will investigate. So we realize the necessity to effectively separate the slow from the fast modes using multi-scale asymptotic perturbation techniques (e.g. Sergey et al., 2004 and Jerzy, 2006). It is also noticed that slow time scale might be taken into account from the governing equations (2.1), which will be of significance when time-modulated waves are considered. Here we only consider waves with a fixed basic period propagating in a wave flume.

3.2 Solving the Evolution Equations

Since the amplitudes a_j are complex quantities, the solution will become simpler if we introduce real quantities even though the number of equations will be doubled. Following Dingemans (1997), splitting a complex function into amplitude and phase, or into the real and imaginary parts, is adopted as two solution techniques.

3.2.1 Solving the Complex Equation Directly

It is intuitive to solve the complex evolution equations (2.8) directly but this requires the capability of coping with complex functions. MATLAB, which has the default declaration and definition for complex arithmetic, will be used to solve the complex equations directly. This will also serve as a reference in comparison with other solution techniques of splitting.

3.2.2 Splitting the Complex Function into Amplitude and Phase Functions

When using the amplitude and phase description, we write

$$a_j(X) = \alpha_j(X)e^{i\varphi_j(X)} \tag{3.1}$$

with j=1, 2, 3 and $\alpha_j(X)$ and $\varphi_j(X)$ real functions. Furthermore, the interaction equations (2.8) and their conjugated equations can be rewritten as

$$\frac{d\alpha_1}{dX} = -T_1\alpha_1\alpha_2\sin\Lambda - S_1\alpha_2\alpha_3\sin\Omega \tag{3.2a}$$

$$\frac{d\alpha_2}{dX} = T_2\alpha_1^2\sin\Lambda - S_2\alpha_1\alpha_3\sin\Omega \tag{3.2b}$$

$$\frac{d\alpha_3}{dX} = S_3\alpha_1\alpha_2\sin\Omega \tag{3.2c}$$

$$\frac{d\varphi_1}{dX} = -T_1\alpha_2\cos\Lambda - S_1\frac{\alpha_2\alpha_3}{\alpha_1}\cos\Omega \tag{3.2d}$$

$$\frac{d\varphi_2}{dX} = -\frac{T_2\alpha_1^2}{\alpha_2}\cos\Lambda - S_2\frac{\alpha_1\alpha_3}{\alpha_2}\cos\Omega \tag{3.2e}$$

$$\frac{d\varphi_3}{dX} = -S_3\frac{\alpha_1\alpha_2}{\alpha_3}\cos\Omega \tag{3.2f}$$

where phase functions are defined as:

$$\Lambda(X) = 2\varphi_1 - \varphi_2 - \Delta k \cdot X \tag{3.3a}$$

$$\Omega(X) = \varphi_1 + \varphi_2 - \varphi_3 - \delta k \cdot X \tag{3.3b}$$

$\alpha_j(X)$ is the spatial variation of amplitudes. However, from the equation forms above, all the harmonics cannot be zero.

3.2.3 Splitting Complex Function into Real and Imaginary Parts

We now set/define

$$a_j(X) = p_j(X) + iq_j(X) \tag{3.4}$$

where j=1, 2, 3, p and q are real. Substitution of equation (3.4) into the complex three-wave evolution equations (2.8) yields

$$\begin{aligned}\frac{dp_1}{dX} = {} & T_1(p_1q_2 - q_1p_2)\cos\vartheta + T_1(p_1p_2 + q_1q_2)\sin\vartheta \\ & + S_1(p_2q_3 - q_2p_3)\cos\upsilon \\ & + S_1(p_2p_3 + q_2q_3)\sin\upsilon\end{aligned} \tag{3.5a}$$

$$\begin{aligned}\frac{dq_1}{dX} = {} & -T_1(p_1p_2 + q_1p_2)\cos\vartheta + T_1(p_1q_2 - q_1p_2)\sin\vartheta \\ & - S_1(p_2p_3 + q_2q_3)\cos\upsilon \\ & + S_1(p_2q_3 - q_2p_3)\sin\upsilon\end{aligned} \tag{3.5b}$$

$$\begin{aligned}\frac{dp_2}{dX} = {} & 2T_2p_1q_1\cos\vartheta - T_2(p_1^2 - q_1^2)\sin\vartheta \\ & + +S_2(p_1q_3 - q_1p_3)\cos\upsilon \\ & + +S_2(p_1p_3 + q_1q_3)\sin\upsilon\end{aligned} \tag{3.5c}$$

$$\begin{aligned}\frac{dq_2}{dX} = {} & -T_2(p_1^2 - q_1^2)\cos\vartheta - 2T_2p_1q_1\sin\vartheta \\ & - S_2(p_1p_3 + q_1q_3)\cos\upsilon \\ & + S_2(p_1q_3 - q_1p_3)\sin\upsilon\end{aligned} \tag{3.5d}$$

$$\frac{dp_3}{dX} = S_3(p_1q_2 + q_1p_2)\cos\vartheta - S_3(p_1p_2 - q_1q_2)\sin\vartheta \tag{3.5e}$$

$$\frac{dq_3}{dX} = -S_3(p_1p_2 - q_1q_2)\cos\vartheta - S_3(p_1q_2 + q_1p_2)\sin\vartheta \tag{3.5f}$$

where $\vartheta = \Delta k \cdot X$ and $\upsilon = \delta k \cdot X$.

Among all these three approaches to solving the evolution equations (2.8), this splitting method has the advantage of programming convenience because it allows complete energy change between harmonics. When the amplitudes of other two harmonics equals to zero, all the wave energy is transferred to the primary wave.

3.3 Numerical Scheme

Madsen and Sørensen (1993) solved the evolution equations numerically by applying a fourth-order Runge-Kutta (RK4) method and obtained sound results. So the same numerical scheme RK4 is employed in solving the evolution equations. The algorithm of RK4 is as below:

Assume the evolution equations (2.8) can be written as

$$\frac{da_j}{dX} = f_j(X, a_j) \tag{3.6}$$

with the boundary condition $a_j^1(X_0) = a_{j0},\ j = 1,2,3$ where X_0 is the starting space grid, a_{j0} are the initial amplitude for each harmonic. Then, the RK4 method for this specific problem is given by the following equations:

$$a_j^{n+1} = a_j^n + \frac{1}{6}dX\left(K_j^n + 2L_j^n + 2M_j^n + N_j^n\right) \tag{3.7a}$$

$$X_{n+1} = X + dX \tag{3.7b}$$

where a_j^{n+1} is the RK4 approximation of $a_j(X_{n+1})$, and

$$K_j^n = f_j\left(X_n, a_j^n\right) \tag{3.8a}$$

$$L_j^n = f_j\left(X_n + \frac{1}{2}dX, a_j^n + \frac{1}{2}dX \cdot K_j^n\right) \tag{3.8b}$$

$$M_j^n = f_j\left(X_n + \frac{1}{2}dX, a_j^n + \frac{1}{2}dX \cdot L_j^n\right) \tag{3.8c}$$

$$N_j^n = f_j\left(X_n + dX, a_j^n + dX \cdot M_j^n\right) \tag{3.8d}$$

where dX is the spatial interval of the slow scale and K, L, M and N are the sloping coefficients.

3.4 Method of Manufactured Solutions (MMS)

3.4.1 MMS in CFD

The Method of Manufactured Solutions (MMS) is a technique by which the numerical algorithm within codes can be verified to ensure that they have been coded correctly and have the capability to solve the equations they claim. The basic ideas of MMS were developed in 1980s, but it was not until around 2003 that MMS began to be applied to large, general-purpose flow solvers. For example, successful applications of MMS have been used to verify numerical schemes for both the inviscid and viscous terms of the Navier-Stokes equations. Also, the method has been extended to cover various turbulence models and boundary conditions.

MMS is a very useful tool for CFD code accuracy verification. If there is a built-in MMS algorithm in a particular CFD code, it would be well worth the time to use it to verify as many of the algorithms you will be using as possible. The basic concept of MMS arose out of recognition that you could determine the order of accuracy for a numerical scheme if you could just get an accurate measure of the errors on any particular computational grid. MMS is used where no exact solutions exist or where exact solutions are not sufficiently general to fully test a code, or where exact solutions are not smooth enough to allow proper implementation and error analysis (Bond et al., 2006).

Unlike exact solutions, the manufactured solutions do not actually have to satisfy the original governing equations for given initial and boundary conditions. Instead, the original equations are modified by addition of source terms so that the manufactured solutions are exact solutions to the modified governing equations. In Patrick (2002) three example problems in MMS were demonstrated on the choice of manufactured solutions. Bond et al. (2005) and Subrahmanya et al. (2010) applied the MMS to test the Euler and Navier-Stokes equations and also used MMS to verify the boundary conditions of CFD codes.

3.4.2 The Procedure of MMS

The specific steps to apply MMS to a particular algorithm will be very code-specific. The general procedure is as follows:

1) Choose the form of the governing equations;
2) Choose the form of the manufactured solutions as simple as possible;
3) Insert the manufactured solutions into the governing equations to lead to additional source terms;
4) Solve the modified governing equations with the source terms;
5) Evaluate the global discretization error in the numerical solutions;
6) Determine the order of accuracy.

If the order of accuracy determined at the end of the last step matches the nominal order of accuracy of your code, everything is fine. If not, it means something is wrong, and further investigation is required.

When implementing MMS in a CFD code, since the manufactured solutions are not actually the result of solving the governing equations (because they are "manufactured"), plugging them into the Euler or Navier-Stokes equations will result in extra nontrivial but known structured terms that do not cancel out the way a true solution would. These terms can, however, be added as source terms to the right hand side of the governing equations to create a modified set of governing equations for which the manufactured solutions are correct. These source terms are quite complex and it might take several pages to print out. So it is important to design the manufactured solutions as simple as possible to make added source terms less complicated.

CHAPTER 4 RESULTS AND DISCUSSION

This chapter first utilizes the method of manufactured solutions (MMS) to verify the code implementation as well as the numerical scheme. Then it examines the results of the one-dimensional Boussinesq-type equations for a specific scenario. The chosen scenario is designed to investigate the accuracy of the developed models expressed by the evolution equations in comparison with the exact solution. Based on the numerical results, experiments of the perturbation parameter effect on the beat length and amplitude are carried out.

4.1 Model Test with MMS

In order to verify the code of solving the evolution equations (2.8), the method of manufactured solutions (MMS) is introduced. A full test equation is designed below using MMS with the wave number mismatch property and the periodic boundary condition. The same harmonic generation scenario on a flat bed as in Chen et al. (1999) is conducted where the wave period T=2.5s, wave height H=0.084m, water depth h=0.4m; initial amplitudes $a_1 = \frac{H}{2}, a_2 = a_3 = 0$; grid spacing dx=0.05m; and the numerical model is tested for 30m of physical distance.

According to the procedure of MMS discussed in Section 3.5.2, the first step is to choose the governing equations, which are the evolution equations (2.8). The second step is then to pick up the form of the manufactured solutions:

$$a_1 = \frac{H}{2} e^{iA_1 X} \cos A_2 X \tag{4.1a}$$

$$a_2 = \frac{H}{5} e^{iB_1 X} \sin B_2 X \tag{4.1b}$$

$$a_3 = \frac{H}{7} e^{iC_1 X} \sin C_2 X \tag{4.1c}$$

where $A_j, B_j, C_j, j = 1,2$ are constant coefficients to be determined later. Inserting the manufactured solutions into the evolution equations generates the source terms

$$\begin{aligned} &\frac{da_1}{dX} + i\frac{Q_1}{S_1} a_1^* a_2 e^{i(\emptyset_2 - 2\emptyset_1)} + i\frac{P_1}{S_1} a_2^* a_3 e^{i(\emptyset_3 - \emptyset_2 - \emptyset_1)} \\ &= \frac{H}{2} e^{iA_1 X}(iA_1)\cos A_2 X - \frac{H}{2} e^{iA_1 X} A_2 \sin A_2 X \\ &+ i\frac{Q_1}{S_1}\frac{H}{2} e^{-iA_1 X}\cos A_2 X \frac{H}{5} e^{iB_1 X}\sin B_2 X e^{i(\emptyset_2 - 2\emptyset_1)} \\ &+ i\frac{P_1}{S_1}\frac{H}{5} e^{-iB_1 X}\sin B_2 X \frac{H}{7} e^{iC_1 X}\sin C_2 X e^{i(\emptyset_3 - \emptyset_2 - \emptyset_1)} = M_1 \end{aligned} \tag{4.2a}$$

$$\begin{aligned} &\frac{da_2}{dX} + i\frac{Q_2}{S_2} a_1^2 e^{i(2\emptyset_1 - \emptyset_2)} + i\frac{P_2}{S_2} a_1^* a_3 e^{i(\emptyset_3 - \emptyset_2 - \emptyset_1)} \\ &= \frac{H}{5} e^{iB_1 X}(iB_1)\sin B_2 X + \frac{H}{5} e^{iB_1 X} B_2 \sin B_2 X \\ &+ i\frac{Q_2}{S_2}\left(\frac{H}{2} e^{iA_1 X}\cos A_2 X\right)^2 e^{i(2\emptyset_1 - \emptyset_2)} \\ &+ i\frac{P_2}{S_2}\frac{H}{2} e^{-iA_1 X}\cos A_2 X \frac{H}{7} e^{iC_1 X}\sin C_2 X e^{i(\emptyset_3 - \emptyset_2 - \emptyset_1)} = M_2 \end{aligned} \tag{4.2b}$$

$$\begin{aligned} &\frac{da_3}{dX} + i\frac{P_3}{S_3} a_1 a_2 e^{i(\emptyset_1 + \emptyset_2 - \emptyset_3)} \\ &= \frac{H}{7}(iC_1) e^{iC_1 X}\sin C_2 X + \frac{H}{7} e^{iC_1 X} C_2 \sin C_2 X \\ &+ i\frac{P_3}{S_3}\frac{H}{2} e^{iA_1 X}\cos A_2 X \frac{H}{5} e^{iB_1 X}\sin B_2 X e^{i(\emptyset_1 + \emptyset_2 - \emptyset_3)} = M_3 \end{aligned} \tag{4.2c}$$

where M_1, M_2 and M_3 are source terms of the modified evolution equations. Therefore, the modified evolution equations becomes

$$\frac{da_1}{dX} = -i\frac{Q_1}{S_1} a_1^* a_2 e^{i(\emptyset_2 - 2\emptyset_1)} - i\frac{P_1}{S_1} a_2^* a_3 e^{i(\emptyset_3 - \emptyset_2 - \emptyset_1)} + M_1 \tag{4.3a}$$

$$\frac{da_2}{dX} = -i\frac{Q_2}{S_2} a_1^2 e^{i(2\emptyset_1 - \emptyset_2)} - i\frac{P_2}{S_2} a_1^* a_3 e^{i(\emptyset_3 - \emptyset_2 - \emptyset_1)} + M_2 \tag{4.3b}$$

$$\frac{da_3}{dX} = -i\frac{P_3}{S_3} a_1 a_2 e^{i(\emptyset_1 + \emptyset_2 - \emptyset_3)} + M_3 \tag{4.3c}$$

For simplicity, we set all the coefficients in the exact solution equal to 1. And then the exact solution becomes:

$$a_1 = \frac{H}{2} e^{iX} \cos X \tag{4.4a}$$

$$a_2 = \frac{H}{5} e^{iX} \sin X \tag{4.4b}$$

$$a_3 = \frac{H}{7} e^{iX} \sin X \tag{4.4c}$$

and

$$M_1 = \frac{H}{2} e^{iX}(i)\cos X - \frac{H}{2} e^{iX} \sin X + i \frac{Q_1}{S_1} \frac{H^2}{10} \cos X \sin X e^{i(\emptyset_2 - 2\emptyset_1)} + i \frac{P_1}{S_1} \frac{H^2}{35} \sin^2 X \, e^{i(\emptyset_3 - \emptyset_2 - \emptyset_1)} \tag{4.5a}$$

$$M_2 = \frac{H}{5} e^{iX}(i)\sin X + \frac{H}{5} e^{iX} \sin X + i \frac{Q_2}{S_2} \left(\frac{H}{2} e^{iX} \cos X\right)^2 e^{i(2\emptyset_1 - \emptyset_2)} + i \frac{P_2}{S_2} \frac{H^2}{14} \cos X \sin X e^{i(\emptyset_3 - \emptyset_2 - \emptyset_1)} \tag{4.5b}$$

$$M_3 = \frac{H}{7} (i) e^{iX} \sin X + \frac{H}{7} e^{iX} \sin X + i \frac{P_3}{S_3} \frac{H^2}{10} e^{i2X} \cos X \sin X e^{i(\emptyset_1 + \emptyset_2 - \emptyset_3)} \tag{4.5c}$$

Now we solve the equations (4.3) with the source terms (4.5).

4.1.1 Results

This MMS test case is for solving the complex equations directly and again the RK4 numerical scheme is applied here. The model results are shown in Fig. 4-1. The solid lines are the numerical results from solving the modified evolution equations (4.3) while the dotted lines represent exact solutions (4.4). The blue denotes the first mode of the solution, and red for the second, and green for the third. Solving the evolution equations by the other two splitting methods discussed before give the same results as directly solving the complex equations.

4.1.2 Discussion

The results show that the numerical result is identical to the exact solution with less than 10^{-6} of relative error. The numerical algorithm RK4 is also demonstrated to be effective to solve the set of differential equations. This therefore verifies the code implementation for solving the evolution equations of triad interaction in shallow water.

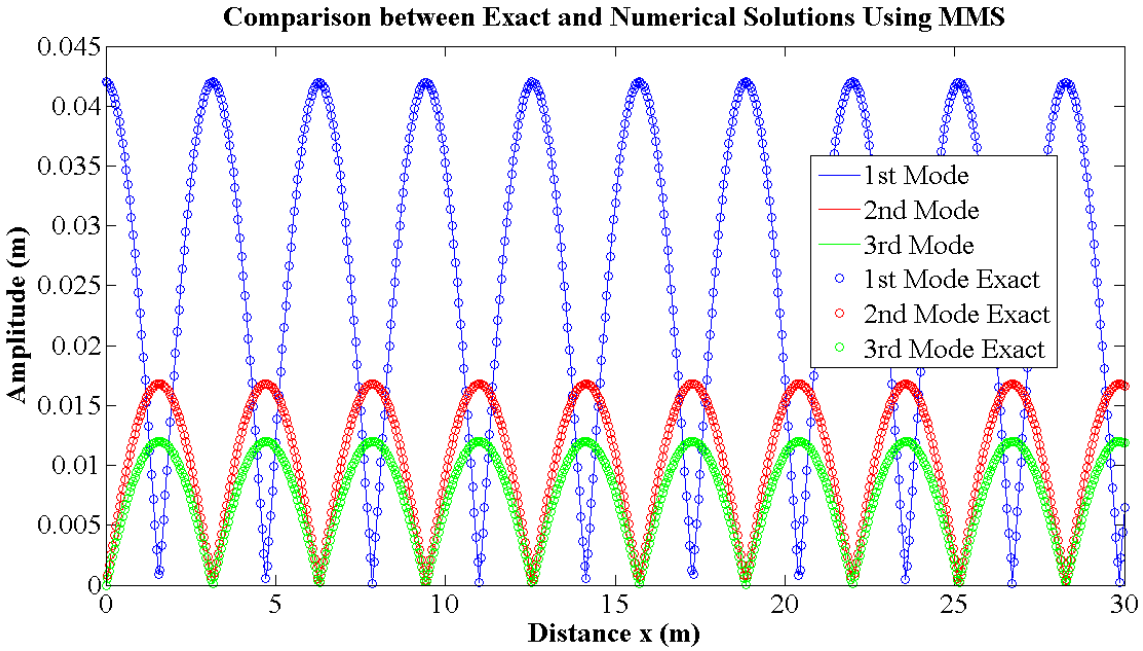

Figure 4-1 Comparison between Exact and Numerical Solutions Using MMS

4.2 Solving the Evolution Equations for Triad Interaction of Shallow Water Waves

The test model using MMS has been able to validate the code correctness of solving the evolution equations (2.8). In this section, we use the RK4 numerical scheme to solve the evolution equations (2.8) by applying three approaches described in Section 3.3. All the other initial and wave conditions are set the same as the case of solving the evolution equations, i.e., the water depth is 0.4m, the first harmonic period is 2.5s and the wave height is 0.084m; the initial amplitudes of the second and third harmonics are zero; the

grid spacing is chosen as 0.05m and the numerical model is tested for 30m physical distance with a periodic boundary condition.

As discussed in Dingemans (1997), the accuracy of the dispersion relationship is important for near-resonant interactions. With respect to high harmonic generation, even if the primary wave satisfies shallow water condition h/L_0, this is not necessary the case for high harmonics and the phase mismatch may be rather inaccurate compared to the exact dispersion relationship if the classic Boussinesq equations are used. Madsen and Sørensen (1993) have showed that the classical Boussinesq equations led to an overestimation of phase mismatch. That is why we chose the Boussinesq-type equations (2.1) with b=1/15 because it provides a significant improvement in the accuracy of the wave number of higher harmonics.

4.2.1 Results

This case is similar to that in Chen et al. (1999). A sinusoidal wave with a period T=2.5s and amplitude of 0.042m was input to the model. The figures below present the results by solving the evolution equations (2.8) for waveform modulation resulting from nonlinear interactions of three wave components. Fig. 4-2 shows the numerical results by solving the evolution equations (2.8) with complex function solutions directly. Fig. 4-3 presents the triad interaction by splitting the complex function into amplitude and phase functions of (3.2). The result by splitting the complex function into real and imaginary parts from (3.5) is demonstrated in Fig. 4-4.

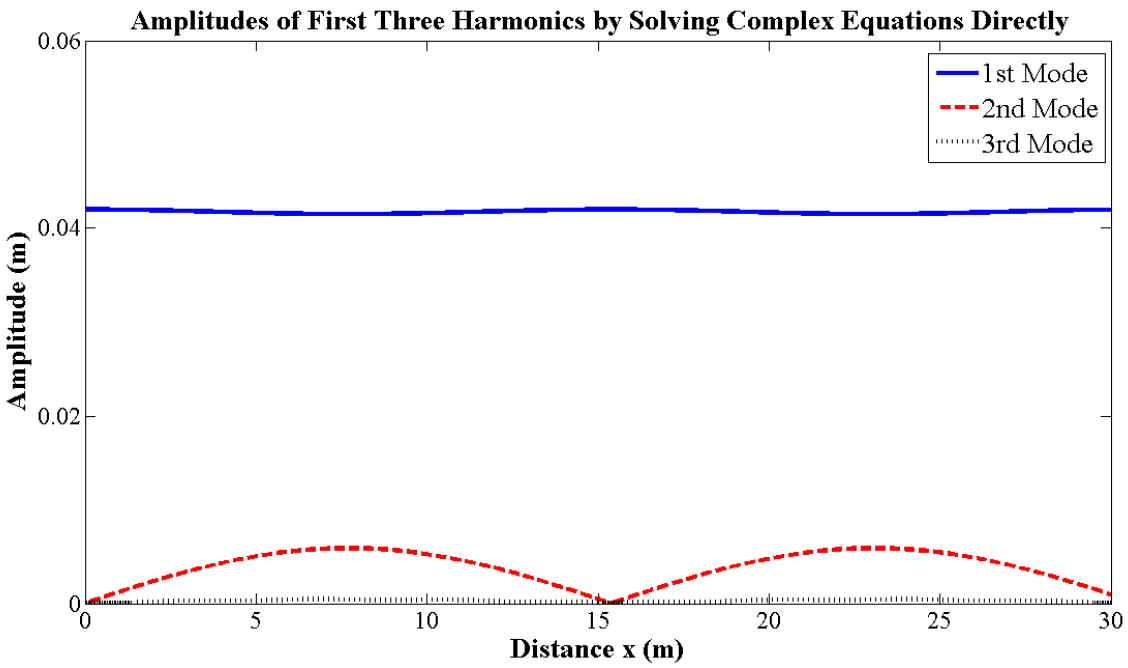

Figure 4-2 Amplitudes of First Three Harmonics by Solving Complex Equations Directly

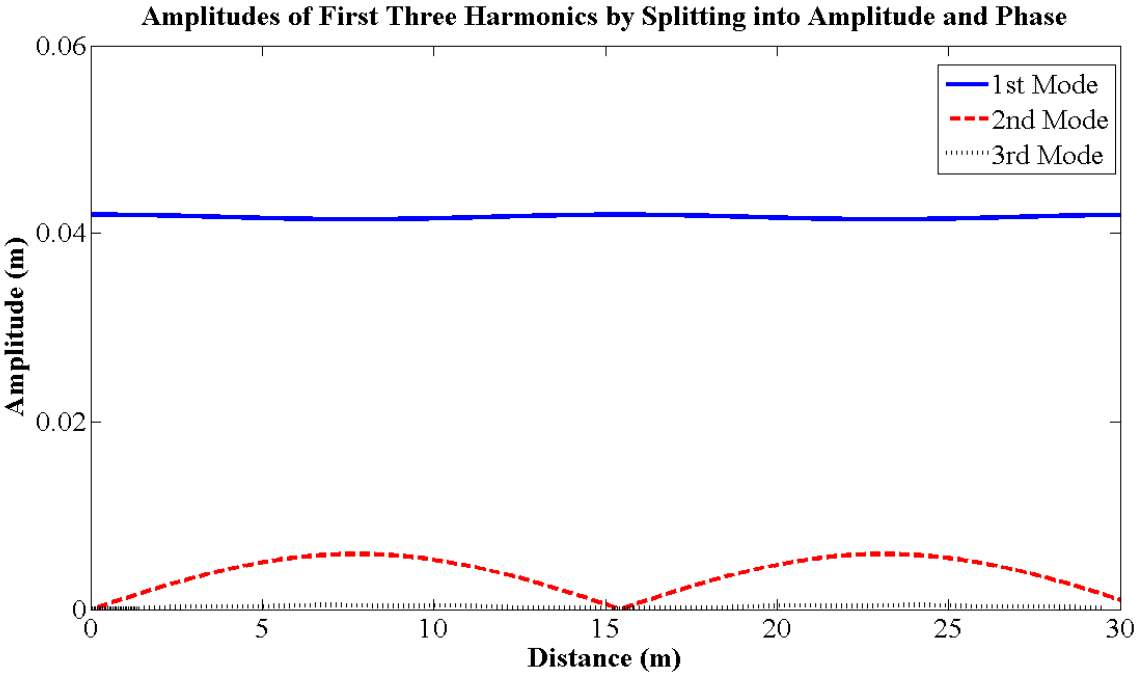

Figure 4-3 Amplitudes of First Three Harmonics by Splitting into Amplitude and Phase

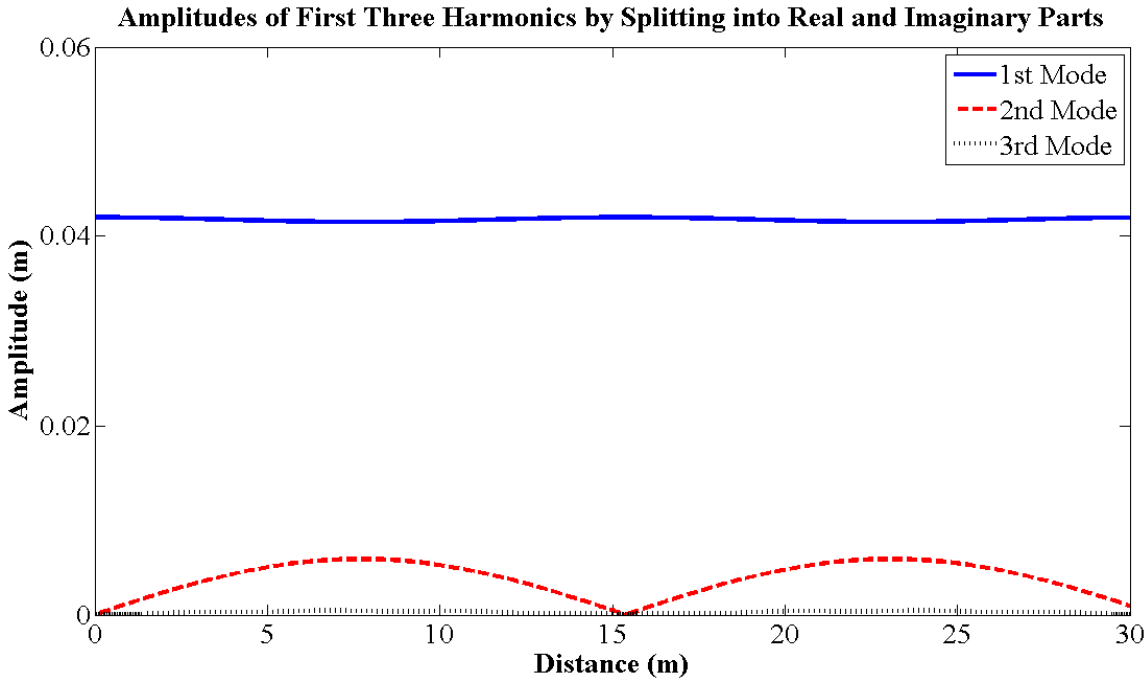

Figure 4-4 Amplitudes of First Three Harmonics by Splitting into Real and Imaginary Parts

4.2.2 Discussion

It is seen that to solve the evolution equations for triad interaction of shallow water waves by the fourth-order Runge-Kutta scheme in three methods (solving complex directly, splitting into amplitude and phase functions and, splitting into real and imaginary parts) gives identical numerical results. However, the wave energy exchange is not very evident among three harmonics, which is much smaller compared with those in Chen et al. (1999) and Kaihatu (2009). Table 4.1 presents the values of beat length and amplitudes for first three components from those two papers. The cross-spectral energy transfers back and forth between the primary wave and high harmonics, showing both papers agree perfectly with each other. As mentioned in literature review in Chapter Two, the numerical results in Chen et al. (1999) are based on the time domain model of Madsen and Schäffer (1998) for wave/current interaction, while Kaihatu's (2009) is

based on the frequency domain model developed by Kaihatu and Kirby (1995). Both models are of much higher dispersion accuracy than Boussinesq-type equations with b=1/15 such that the corresponding numerical results can be regarded as the "exact" solution. Therefore a further research on the difference between results is continued.

Table 4.1 Beat Length and Amplitude of Each Harmonics from Chen et al. (1999)

Beat length (m)	a_1^{max} (m)	a_1^{min} (m)	a_2^{max} (m)
13.9403	0.042	0.034579	0.021981

4.3 Influence of Perturbation Parameter on Numerical Results

An interest arose in finding out the reason of difference between numerical results and exact solutions. In this section, we repeat the tests with the same initial and boundary conditions, but replace the nonlinear parameter $\epsilon = \frac{a_1}{h} = 0.105$ with a perturbation parameter, which can be set freely to see its influence on the numerical results. Nine experiments with different choices of perturbation parameter ranging from 0.1 to 0.5 with interval of 0.05 have been conducted. Considering the amplitude variation of each harmonics, the first two wave components are taken into account.

4.3.1 Results

Table 4.2 presents the model results in terms of the beat length and amplitude variation of the first two harmonics. As in Madsen and Sørensen (1993), the variation of the beat length and maximum amplitude of the second harmonic in terms of perturbation parameter are given in Fig. 4-5.

Table 4.2 Influence of Perturbation Parameter ε on Beat Length and Amplitudes

ε	L_b (m)	a_1^{max} (m)	a_1^{min} (m)	a_2^{max} (m)
0.1	15.3845	0.042	0.0416	0.0056
0.15	15.3471	0.042	0.0410	0.0084
0.2	15.2645	0.042	0.0402	0.011
0.25	15.1225	0.042	0.0393	0.0135
0.3	14.6327	0.042	0.0382	0.0159
0.35	14.6327	0.042	0.037	0.018
0.4	14.3024	0.042	0.0357	0.02
0.45	**13.9424**	**0.042**	**0.0343**	**0.0217**
0.5	13.4523	0.042	0.0330	0.0232
Exact Solution	**13.9403**	**0.042**	**0.034579**	**0.021981**

4.3.2 Discussion

It can be seen from the figure that the perturbation parameter does have effects on the three-wave interaction. The variation of the mean beat length in terms of perturbation parameter ε is monotonically decreasing, while the amplitude is increasing in contrast. When ε=0.45, the beat length and the maximum amplitude of the second harmonic both arrive at the values corresponding to exact solutions. Consequently, we plot the three

wave interaction for the case ε=0.45 in Fig. 4.6, which is in close agreement with the results in Chen et al. (1999) and Kaihatu (2009).

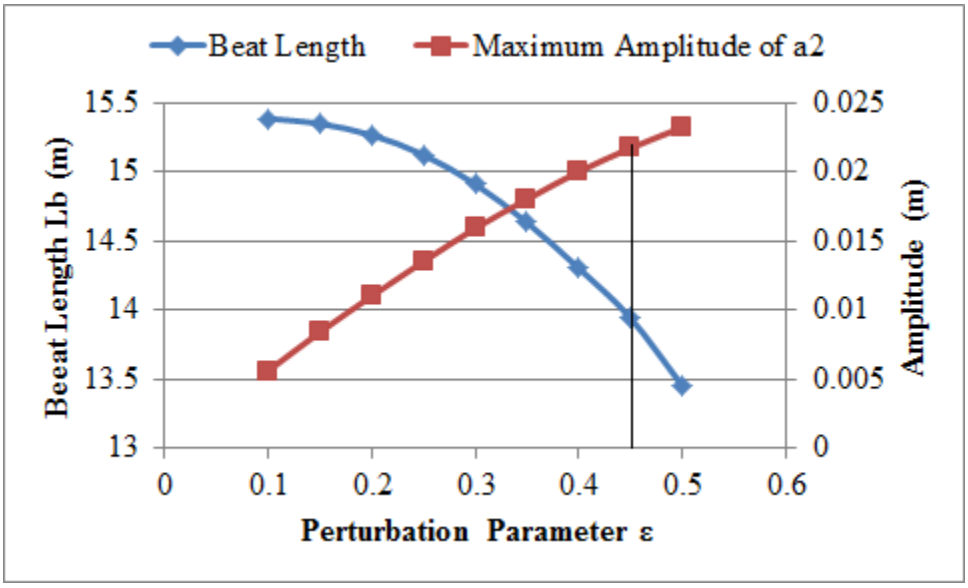

Figure 4-5 Variation of the Beat Length and Amplitude in terms of Perturbation Parameter ε

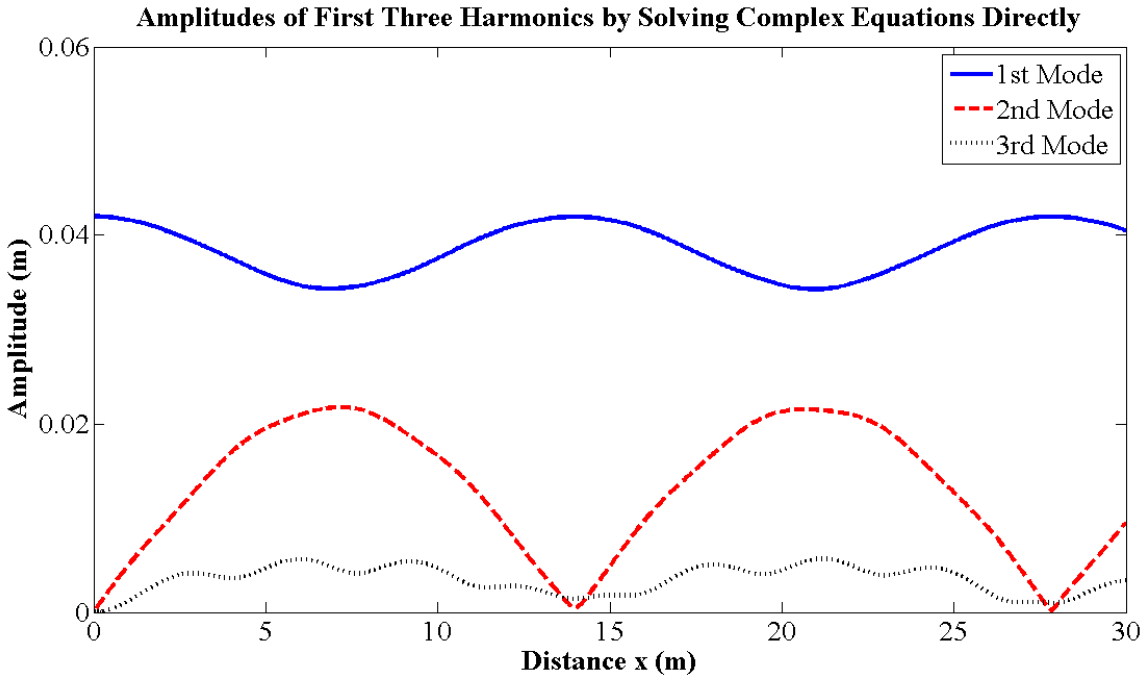

Figure 4-6 Amplitudes of First Three Harmonics with Perturbation Parameter ε=0.45

The nonlinear parameter (ε) in the evolution equations, which is the ratio of wave amplitude to still water depth, is not necessarily the perturbation parameter. Although an optimal choice of the perturbation parameter other than ε is yet to be determined, this study is the first to discover that the accuracy of the evolution equations for triad interaction strongly depends on the perturbation parameter in comparison with the exact solution Perfect agreement may be achieved with an appropriate choice of the parameter.

CHAPTER 5 SUMMARY AND RECOMMENDATION

5.1 Summary

Triad interaction of water waves in shallow water are important for a number of physical processes and to explain the energy transfer between low and high frequency parts of the wave spectra during wave propagation. The strength of energy transfer is determined by the phase mismatch between bound and free wave numbers, implying that the accuracy of the dispersion relationship of the governing equation is essential in modeling this phenomenon.

Inspired by Chen et al. (1999), the evolution equations based on the Boussinesq-type equations were derived using the multi-scale perturbation analysis. With the help of Dingemans (1997), the evolution equations were solved to simulate nonlinear triad interaction of shallow water waves by three approaches plus a fourth-order Runge-Kutta (RK4) scheme.

The model results show spatial variation of the amplitudes but the energy transfers among the wave components are underestimated compared to Chen et al. (1999) and Kaihatu(2009). The perturbation parameter effect on triad interaction required further testing and it was found that both the beat length and amplitude of the second harmonic are greatly affected by the perturbation parameter. In particular, when the perturbation parameter ε=0.45, the numerical results are very close to the exact solutions.

Another useful tool to verify nonlinear models is the Method of Manufactured Solutions (MMS), which can be used to test the numerical code. The greatest advantage of MMS is that it enables the programmer to build up an analytical solution at ease and

make it the exact solution to the new modified governing equations with added source terms. The manufactured solutions were then designed in the study to serve as the exact solutions to the derived evolution equations. The same numerical method and wave condition were utilized for the modified equations, yielding the solutions with less than 10^{-6} order of error in comparison with the manufactured exact solution. This validates the correctness of the algorithm and numerical scheme in solving the original evolution equations for triad interaction implemented in this study.

5.2 Recommendation for Future Work

Even though the perturbation parameter effect on energy transfer among harmonic generation has been investigated and the choice of ε=0.45 has been tested to be the optimal value for the case simulated, it is still unknown how the parameter varies with different wave conditions. More wave conditions should be simulated to compare with the exact solutions from time domain and/or frequency domain models in Chen et al. (1999) and Kaihatu's (2009), respectively. An effective algorithm for choosing an optimal perturbation parameter needs to be developed.

Although solving the evolution equations for triad interaction of shallow water waves provides insight into the physical mechanism and improves the understanding of the phenomenon, the evolution equations prove not accurate enough to simulate nonlinear triad interaction. So one recommendation is to involve more harmonics into the evolution equations in order to enhance the wave energy exchange among wave components. On the other hand, time domain numerical models for solving the fully-nonlinear Boussinesq-type equations need to be used for future studies with the help of high-performance computing technologies. Cactus is a framework containing a generic parallel

computational toolkit designed for high-performance computing. Implementing Boussinesq-type models with wind stresses, bottom shear stresses, Corriolis force and diffusion terms into Cactus for large-scale simulations needs to be pursued. This will provide us with a powerful tool to study the effects of wind, current, and vegetation on nearshore wave transformation and triad interaction of nonlinear waves in a deltaic coastal environment.

REFERENCES

Armstrong, J. A., N. Bloembergen, J. Ducuing, and P. S. Pershan.,1962. Interactions between light waves in a nonlinear dielectric. Phys. Rev., 127, 1918-1939.

Bond, R. B., Knupp, P. M., and Ober, C. C., 2005. A manufactured solution for verifying CFD boundary conditions, Part II. 43rd AIAA Paper, 2005-0088.

Bond, R. B., Ober, C. C., and Knupp, P. M., 2006. A manufactured solution for verifying CFD boundary conditions, Part III. AIAA Paper, 2006-3722.

Bretherton, F. P., 1964. Resonant interactions between waves: The case of discrete oscillation. J. Fluid Mech., 20, 457-480.

Bryant, P. J., 1973. Periodic waves in shallow water. J. Fluid Mech., 59 (4), 625-644.

Bryant, P. J., 1983. Waves and wave groups in deep water. In: Nonlinear Waves, 100-115, Cambridge Univ. Press.

Buhr-Hansen, J. and Svendsen, I. A., 1974. Laboratory generation of waves of constant forms. In 14th Coastal Engineering Conference, June 1974, Copenhagen, Ch. 18, 320-338.

Chen, Q., Madsen, P. A., Schäffer, H. A., Basco, D. R., 1998. Wave–current interaction based on an enhanced Boussinesq approach. Coast. Eng., 33, 11–39.

Chen, Q., Madsen, P. A., Basco, D. R., 1999. Current effects on nonlinear interactions of shallow-water waves. J. Wtrwy., Port, and Oc. Engrg., 125, 176-186.

Chapalain, G., Cointe, R. and Temperville, A., 1992. Observed and modeled resonantly interacting progressive water waves. Coastal Engrg., 16, 267-301.

Dingemans, M. W., 1997. Water wave propagation over uneven bottoms. Part 2-Nonlinear wave propagation. World Scientific, River Edge, N. J., 806-814.

Elgar, S., Freilich, M. H., and Guza, R. T., 1990. Recurrence in truncated Boussinesq models for nonlinear waves in shallow water. J. Oceanography., 95, 11547-11556.

Freilich, M. H., and Guza, R. T., 1984. Nonlinear effects on shoaling surface gravity waves. Philosophical Trans. Royal Soc., London, A331, 1-41.

Goda, Y., 1967. Travelling secondary wave in channels. Port and Harbor Research Institute, Ministry of Transport, Japan., Report 13, 32-38.

Galvin, C. J., Jr., 1968. Breaker type classification on three laboratory beaches. J. Geophys Res., 73, 3651-3659.

Kaihatu, J. M., 2001. Improvement of parabolic nonlinear dispersive wave model. J. Wtrwy. Port. Coast. Ocean Eng., 127, 113-121.

Kaihatu. J. M., 2009. Application of a nonlinear frequency domain wave-current interaction model to shallow water recurrence effects in random waves. Ocean Modeling., 26, 190–205.

Kaihatu. J. M, Kirby, J. T., 1995. Nonlinear transformation of waves in finite water depth. Phys. Fluids., 7, 1903-1914.

Kirby, J. T., 1991. Intercomparison of truncated series solutions for shallow water waves. J. of Waterway, Port, Coastal, and Ocean Engineering., 8 (3), 219-232.

Kristensen, M. K., 1995. Boussinesq equations and wave-current interaction. M.Sc. thesis. International Research Center for Computational Hydrodynamics (ICCH) at Danish Hydraulic Institute, Denmark and ISVA, Technical University of Denmark.

Madsen, P. A., Murray, R., Sørensen, O. R., 1991. A new form of the Boussinesq equations with improved linear dispersion characteristics (part 1). Coastal Eng., 15, 371-388.

Madsen, P. A., and Sørensen, O. R., 1993. Bound waves and triad interactions in shallow water. Oc. Engrg., 20, 359–388.

Madsen, P. A., and Schäffer, H.A., 1998. Higher order Boussinesq-type equations: Derivation and analysis. Philosophical Trans. Royal society, London, U.K., A356, 3123-3184.

Mei, C.-C., 1989. The applied dynamics of ocean surface waves. World Scientific.

Mei, C.-C, Ünlüata, U., 1972. Harmonic generation in shallow water waves. In: Meyer, R.E. (Ed.), Waves on Beaches. Academic Press, New York., 181-202.

Nayfeh A. H., 1978. Perturbation theory, A Willy Interscience Publ.

Nwogu, O., 1993. Alternative form of Boussinesq equations for nearshore wave propagation. J. Waterw. Port Coastal Ocean Eng. ASCE., 119 (6), 619-638.

Patrick, J. Roache., 2002. Code verification by the method of manufactured solutions. Transactions of the ASME., 124 (4), 4-10.

Peregrine, D.H., 1967. Long waves on a beach. J. Fluid Mech., 27(4), 815-827.

Prüser, H. H., Zielke, W., 1990. Irregular waves on a current. In: Proc. 22nd Int. Conf. Coastal Eng., vol. 1. Delft, The Netherlands and ASCE, New York., 1088-1101.

Rayleigh, L., 1927. The theory of sound, vol.I. London.

Rellich, F., 1936. Störumgstheory der Spektralzerlegung, I, Math. Ann., 113, 600-619.

Schäffer, H. A., Madsen, P. A., 1995. Further enhancements of Boussinesq-type equations. Coastal Eng., 26, 1-14.

Schrödinger, E., 1926. Quantisierung als Eigenwertproblem, Ann. Physik., 80, 437-490.

Sergey K. Nemirovskii and Sergey A. Ponomarenko., 2004. Multi-scale perturbation analysis in hydrodynamics of the superfluid turbulence. Derivation of the Dresner equation., eprint arXiv:cond-mat/0412420.

Subrahmanya P. Veluri and Christopher J. Roy., 2010. Comprehensive code verification for an unstructured finite volume CFD code. AIAA Paper., 2010-127.

Witting, J. M., 1984. A unified model for the evolution of nonlinear water waves. J. of Computational Physics., 56 (2), 203-236.

Won, Y. S. and Battjes, J. A., 1992. Spectral Boussinesq modeling of random waves. Communications on Hydraulic and Geotechnical Engineering., 27.

Yoon, S. B., Liu, P. L. F., 1989. Interaction of currents and weakly nonlinear water waves in shallow water. J. Fluid Mech., 205. 397-419.

APPENDIX A: MATLAB CODE FOR SOLVING THE EVOLUTION EQUATIONS DIRECTLY

```
% RK4 solving complex a(X) for the evolution equations
clear,clc
T=2.5;   % unit: s
H=0.084; % unit: m
h=0.4;   % water depth unit: m
% dt=0.01;  % unit: s
dx=0.05; % unit: m
w0=2*pi/T;
w=[w0,2*w0,3*w0];
g=9.81;
% b=0;
b=1/15;
k=sqrt(((1/3+b)*h^2*w.^2-g*h+sqrt(((1/3+b)*h^2*w.^2-
g*h).^2+4*b*g*w.^2*h^3))/(2*b*g*h^3)); %when b=1/15 from eqn.(5.122) on book
p.524
x=0:dx:30;
n=length(x);

%initial condition (western boundary)
a1=H/2;
a2=0;
a3=0;
epsilon=0.45;
X=epsilon*x;
dX=dx*epsilon;

%initialize a
a=zeros(3,n);
a(1,1)=a1;
a(2,1)=a2;
a(3,1)=a3;
for j=1:3
   a(j,end)=a(j,1); %periodic BC
end

%set S,P and Q
Q1=g/h*(k(2)-k(1))^2*(w(1)/k(1)+w(2)/k(2))+1/h^2*w(1)*w(2)*(w(2)-w(1))*(1/k(1)-
1/k(2));
Q2=2/h^2.*w(1)^3/k(1)+4*g/h*k(1)*w(1);
P1=g/h*(k(3)-k(2))^2*(w(2)/k(2)+w(3)/k(3))+1/h^2*w(2)*w(3)*(w(3)-w(2))*(1/k(2)-
1/k(3));
P2=g/h*(k(3)-k(1))^2*(w(1)/k(1)+w(3)/k(3))+1/h^2*w(1)*w(3)*(w(3)-w(1))*(1/k(1)-
1/k(3));
```

```
P3=g/h*(k(1)+k(2))^2*(w(1)/k(1)+w(2)/k(2))+1/h^2*w(1)*w(2)*(w(1)+w(2))*(1/k(1)+1
/k(2));
S=2*g*w.*(1-h/g.*w.^2*(1/3+b)+3*b*h^2.*k.^2/2);

atemp=zeros(size(a));
phitemp=zeros(size(a));

%solve a1,a2,a3 from eqn (29)-(31) using RK4
for j=1:n-1
   phi(1,:)=k(1)*X/epsilon;
   phi(2,:)=k(2)*X/epsilon;
   phi(3,:)=k(3)*X/epsilon;
   %   set KK1
   KK1(1,j)=-i*(Q1/S(1)*a(1,j)'*a(2,j)*exp(i*(phi(2,j)-
2*phi(1,j)))+P1/S(1)*a(2,j)'*a(3,j)*exp(i*(phi(3,j)-phi(2,j)-phi(1,j))));
   KK1(2,j)=-i*(Q2/S(2)*(a(1,j))^2*exp(i*(2*phi(1,j)-
phi(2,j)))+P2/S(2)*a(1,j)'*a(3,j)*exp(i*(phi(3,j)-phi(2,j)-phi(1,j))));
   KK1(3,j)=-i*P3/S(3)*a(1,j)*a(2,j)*exp(i*(phi(1,j)+phi(2,j)-phi(3,j)));
   atemp(1,j)=a(1,j)+1/2*dX*KK1(1,j);
   atemp(2,j)=a(2,j)+1/2*dX*KK1(2,j);
   atemp(3,j)=a(3,j)+1/2*dX*KK1(3,j);
   phitemp(1,j)=k(1)*(X(j)+1/2*dX)/epsilon;
   phitemp(2,j)=k(2)*(X(j)+1/2*dX)/epsilon;
   phitemp(3,j)=k(3)*(X(j)+1/2*dX)/epsilon;
   %   set KK2
   KK2(1,j)=-i*(Q1/S(1)*atemp(1,j)'*atemp(2,j)*exp(i*(phitemp(2,j)-
2*phitemp(1,j)))+P1/S(1)*atemp(2,j)'*atemp(3,j)*exp(i*(phitemp(3,j)-phitemp(2,j)-
phitemp(1,j))));
   KK2(2,j)=-i*(Q2/S(2)*(atemp(1,j))^2*exp(i*(2*phitemp(1,j)-
phitemp(2,j)))+P2/S(2)*atemp(1,j)'*atemp(3,j)*exp(i*(phitemp(3,j)-phitemp(2,j)-
phitemp(1,j))));
   KK2(3,j)=-i*P3/S(3)*atemp(1,j)*atemp(2,j)*exp(i*(phitemp(1,j)+phitemp(2,j)-
phitemp(3,j)));
   atemp(1,j)=a(1,j)+1/2*dX*KK2(1,j);
   atemp(2,j)=a(2,j)+1/2*dX*KK2(2,j);
   atemp(3,j)=a(3,j)+1/2*dX*KK2(3,j);
   phitemp(1,j)=k(1)*(X(j)+1/2*dX)/epsilon;
   phitemp(2,j)=k(2)*(X(j)+1/2*dX)/epsilon;
   phitemp(3,j)=k(3)*(X(j)+1/2*dX)/epsilon;
   %   set KK3
   KK3(1,j)=-i*(Q1/S(1)*atemp(1,j)'*atemp(2,j)*exp(i*(phitemp(2,j)-
2*phitemp(1,j)))+P1/S(1)*atemp(2,j)'*atemp(3,j)*exp(i*(phitemp(3,j)-phitemp(2,j)-
phitemp(1,j))));
   KK3(2,j)=-i*(Q2/S(2)*(atemp(1,j))^2*exp(i*(2*phitemp(1,j)-
phitemp(2,j)))+P2/S(2)*atemp(1,j)'*atemp(3,j)*exp(i*(phitemp(3,j)-phitemp(2,j)-
phitemp(1,j))));
```

```
   KK3(3,j)=-i*P3/S(3)*atemp(1,j)*atemp(2,j)*exp(i*(phitemp(1,j)+phitemp(2,j)-
phitemp(3,j)));
   atemp(1,j)=a(1,j)+dX*KK3(1,j);
   atemp(2,j)=a(2,j)+dX*KK3(2,j);
   atemp(3,j)=a(3,j)+dX*KK3(3,j);
   phitemp(1,j)=k(1)*(X(j)+dX)/epsilon;
   phitemp(2,j)=k(2)*(X(j)+dX)/epsilon;
   phitemp(3,j)=k(3)*(X(j)+dX)/epsilon;
   % set KK4
   KK4(1,j)=-i*(Q1/S(1)*atemp(1,j)'*atemp(2,j)*exp(i*(phitemp(2,j)-
2*phitemp(1,j)))+P1/S(1)*atemp(2,j)'*atemp(3,j)*exp(i*(phitemp(3,j)-phitemp(2,j)-
phitemp(1,j))));
   KK4(2,j)=-i*(Q2/S(2)*(atemp(1,j))^2*exp(i*(2*phitemp(1,j)-
phitemp(2,j)))+P2/S(2)*atemp(1,j)'*atemp(3,j)*exp(i*(phitemp(3,j)-phitemp(2,j)-
phitemp(1,j))));
   KK4(3,j)=-i*P3/S(3)*atemp(1,j)*atemp(2,j)*exp(i*(phitemp(1,j)+phitemp(2,j)-
phitemp(3,j)));
   % calculate a
   a(1,j+1)=a(1,j)+1/6*dX*(KK1(1,j)+2*KK2(1,j)+2*KK3(1,j)+KK4(1,j));
   a(2,j+1)=a(2,j)+1/6*dX*(KK1(2,j)+2*KK2(2,j)+2*KK3(2,j)+KK4(2,j));
   a(3,j+1)=a(3,j)+1/6*dX*(KK1(3,j)+2*KK2(3,j)+2*KK3(3,j)+KK4(3,j));
end
% BC
for j=1:3
      a(j,end)=a(j,1); %with periodical boundary condition
end

aa1=sqrt((real(a(1,:))).^2+(imag(a(1,:))).^2);
aa2=sqrt((real(a(2,:))).^2+(imag(a(2,:))).^2);
aa3=sqrt((real(a(3,:))).^2+(imag(a(3,:))).^2);
figure
plot(x,aa1);
hold on
plot(x,aa2,'r');
hold on
plot(x,aa3,'k');
xlabel('Distance x (m)'),ylabel('Amplitude (m)'),title('Amplitudes of First Three
Harmonics by Solving Complex Equations Directly')
legend('1st Mode','2nd Mode','3rd Mode')
axis([0 30 0 0.06])
```

APPENDIX B: MATLAB CODE FOR SOLVING THE EVOLUTION EQUATIONS BY SPLITTING THE COMPLEX FUNCTION INTO AMPLITUDE AND PHASE FUNCTIONS

```
% RK4 real equation a(X) solver for the evolution equations
%using a(X)=alpha(X)*exp(i*phi(X)) to split a(X).
clear,clc
h=0.4;
T=2.5;
g=9.81;
H=0.084;
a1=H/2;
a2=1e-10;
a3=1e-10;
epsilon=a1/h;
% epsilon=0.45;
dx=0.05*epsilon;
x=0:dx:30*epsilon;
n=length(x);
alpha1=zeros(size(x));
alpha2=zeros(size(x));
alpha3=zeros(size(x));
phi1=zeros(size(x));
phi2=zeros(size(x));
phi3=zeros(size(x));
alpha1(1)=a1;
alpha2(1)=a2;
alpha3(1)=a3;
alpha1tmp=zeros(size(x));
alpha2tmp=zeros(size(x));
alpha3tmp=zeros(size(x));
phi1tmp=zeros(size(x));
phi2tmp=zeros(size(x));
phi3tmp=zeros(size(x));
w0=2*pi/T;
w=[w0,2*w0,3*w0];
b=1/15;
k=sqrt(((1/3+b)*h^2*w.^2-g*h+sqrt(((1/3+b)*h^2*w.^2-
g*h).^2+4*b*g*w.^2*h^3))/(2*b*g*h^3)); %when b=1/15 from eqn.(5.122) on book
p.524
%set S,P and Q
S=2*g.*w.*(1-h*w.^2/g*(1/3+b)+3*b*h^2*k.^2/2);
Q1=g*(k(2)-k(1))^2*(w(1)/k(1)+w(2)/k(2))/h+w(1)*w(2)*(1/k(1)-1/k(2))*(w(2)-
w(1))/h^2;
P1=g*(k(3)-k(2))^2*(w(3)/k(3)+w(2)/k(2))/h+w(3)*w(2)*(1/k(2)-1/k(3))*(w(3)-
w(2))/h^2;
Q2=4*g*w(1)*k(1)/h+2*(w(1))^3/k(1)/h^2;
```

```
P2=g*(k(3)-k(1))^2*(w(3)/k(3)+w(1)/k(1))/h+w(3)*w(1)*(1/k(1)-1/k(3))*(w(3)-
w(1))/h^2;
P3=g*(k(1)+k(2))^2*(w(1)/k(1)+w(2)/k(2))/h+w(1)*w(2)*(1/k(2)+1/k(1))*(w(1)+w(2))/
h^2;
T1=Q1./S(1);
T2=Q2./S(2);
S1=P1./S(1);
S2=P2./S(2);
S3=P3./S(3);
dk=(k(2)-2*k(1))/epsilon;
deltak=(k(3)-k(2)-k(1))/epsilon;
theta=2*phi1-phi2-dk*x;
omega=phi1+phi2-phi3-deltak*x;
thetatmp=zeros(size(x));
omegatmp=zeros(size(x));

for j=1:n-1
   %     set k1
   k1(1,j)=-(T1*alpha1(j)*alpha2(j)*sin(theta(j))+S1*alpha2(j)*alpha3(j)*sin(omega(j)));
   k1(2,j)=T2*alpha1(j)^2*sin(theta(j))-S2*alpha1(j)*alpha3(j)*sin(omega(j));
   k1(3,j)=S3*alpha1(j)*alpha2(j)*sin(omega(j));
   k1(4,j)=-(T1*alpha2(j)*cos(theta(j))+S1*alpha2(j)*alpha3(j)/alpha1(j)*cos(omega(j)));
   k1(5,j)=-T2*alpha1(j)^2/alpha2(j)*cos(theta(j))-
S2*alpha1(j)*alpha3(j)/alpha2(j)*cos(omega(j));
   k1(6,j)=-S3*alpha1(j)*alpha2(j)/alpha3(j)*cos(omega(j));
   alpha1tmp(j)=alpha1(j)+1/2*dx*k1(1,j);
   alpha2tmp(j)=alpha2(j)+1/2*dx*k1(2,j);
   alpha3tmp(j)=alpha3(j)+1/2*dx*k1(3,j);
   phi1tmp(j)=phi1(j)+1/2*dx*k1(4,j);
   phi2tmp(j)=phi2(j)+1/2*dx*k1(5,j);
   phi3tmp(j)=phi3(j)+1/2*dx*k1(6,j);
   thetatmp(j)=2*phi1tmp(j)-phi2tmp(j)-dk*(x(j)+dx/2);
   omegatmp(j)=phi1tmp(j)+phi2tmp(j)-phi3tmp(j)-deltak*(x(j)+dx/2);
   %     set k2
   k2(1,j)=-
(T1*alpha1tmp(j)*alpha2tmp(j)*sin(thetatmp(j))+S1*alpha2tmp(j)*alpha3tmp(j)*sin(om
egatmp(j)));
   k2(2,j)=T2*alpha1tmp(j)^2*sin(thetatmp(j))-
S2*alpha1tmp(j)*alpha3tmp(j)*sin(omegatmp(j));
   k2(3,j)=S3*alpha1tmp(j)*alpha2tmp(j)*sin(omegatmp(j));
   k2(4,j)=-
(T1*alpha2tmp(j)*cos(thetatmp(j))+S1*alpha2tmp(j)*alpha3tmp(j)/alpha1tmp(j)*cos(om
egatmp(j)));
   k2(5,j)=-T2*alpha1tmp(j)^2/alpha2tmp(j)*cos(thetatmp(j))-
S2*alpha1tmp(j)*alpha3tmp(j)/alpha2tmp(j)*cos(omegatmp(j));
   k2(6,j)=-S3*alpha1tmp(j)*alpha2tmp(j)/alpha3tmp(j)*cos(omegatmp(j));
```

```
   alpha1tmp(j)=alpha1(j)+1/2*dx*k2(1,j);
   alpha2tmp(j)=alpha2(j)+1/2*dx*k2(2,j);
   alpha3tmp(j)=alpha3(j)+1/2*dx*k2(3,j);
   phi1tmp(j)=phi1(j)+1/2*dx*k2(4,j);
   phi2tmp(j)=phi2(j)+1/2*dx*k2(5,j);
   phi3tmp(j)=phi3(j)+1/2*dx*k2(6,j);
   thetatmp(j)=2*phi1tmp(j)-phi2tmp(j)-dk*(x(j)+dx/2);
   omegatmp(j)=phi1tmp(j)+phi2tmp(j)-phi3tmp(j)-deltak*(x(j)+dx/2);
   %     set k3
   k3(1,j)=-
(T1*alpha1tmp(j)*alpha2tmp(j)*sin(thetatmp(j))+S1*alpha2tmp(j)*alpha3tmp(j)*sin(om
egatmp(j)));
   k3(2,j)=T2*alpha1tmp(j)^2*sin(thetatmp(j))-
S2*alpha1tmp(j)*alpha3tmp(j)*sin(omegatmp(j));
   k3(3,j)=S3*alpha1tmp(j)*alpha2tmp(j)*sin(omegatmp(j));
   k3(4,j)=-
(T1*alpha2tmp(j)*cos(thetatmp(j))+S1*alpha2tmp(j)*alpha3tmp(j)/alpha1tmp(j)*cos(om
egatmp(j)));
   k3(5,j)=-T2*alpha1tmp(j)^2/alpha2tmp(j)*cos(thetatmp(j))-
S2*alpha1tmp(j)*alpha3tmp(j)/alpha2tmp(j)*cos(omegatmp(j));
   k3(6,j)=-S3*alpha1tmp(j)*alpha2tmp(j)/alpha3tmp(j)*cos(omegatmp(j));
   alpha1tmp(j)=alpha1(j)+dx*k3(1,j);
   alpha2tmp(j)=alpha2(j)+dx*k3(2,j);
   alpha3tmp(j)=alpha3(j)+dx*k3(3,j);
   phi1tmp(j)=phi1(j)+dx*k3(4,j);
   phi2tmp(j)=phi2(j)+dx*k3(5,j);
   phi3tmp(j)=phi3(j)+dx*k3(6,j);
   thetatmp(j)=2*phi1tmp(j)-phi2tmp(j)-dk*(x(j)+dx);
   omegatmp(j)=phi1tmp(j)+phi2tmp(j)-phi3tmp(j)-deltak*(x(j)+dx);
   %     set k4
   k4(1,j)=-
(T1*alpha1tmp(j)*alpha2tmp(j)*sin(thetatmp(j))+S1*alpha2tmp(j)*alpha3tmp(j)*sin(om
egatmp(j)));
   k4(2,j)=T2*alpha1tmp(j)^2*sin(thetatmp(j))-
S2*alpha1tmp(j)*alpha3tmp(j)*sin(omegatmp(j));
   k4(3,j)=S3*alpha1tmp(j)*alpha2tmp(j)*sin(omegatmp(j));
   k4(4,j)=-
(T1*alpha2tmp(j)*cos(thetatmp(j))+S1*alpha2tmp(j)*alpha3tmp(j)/alpha1tmp(j)*cos(om
egatmp(j)));
   k4(5,j)=-T2*alpha1tmp(j)^2/alpha2tmp(j)*cos(thetatmp(j))-
S2*alpha1tmp(j)*alpha3tmp(j)/alpha2tmp(j)*cos(omegatmp(j));
   k4(6,j)=-S3*alpha1tmp(j)*alpha2tmp(j)/alpha3tmp(j)*cos(omegatmp(j));
   %     calculate a
   alpha1(j+1)=alpha1(j)+1/6*dx*(k1(1,j)+2*k2(1,j)+2*k3(1,j)+k4(1,j));
   alpha2(j+1)=alpha2(j)+1/6*dx*(k1(2,j)+2*k2(2,j)+2*k3(2,j)+k4(2,j));
   alpha3(j+1)=alpha3(j)+1/6*dx*(k1(3,j)+2*k2(3,j)+2*k3(3,j)+k4(3,j));
```

```
    phi1(j+1)=phi1(j)+1/6*dx*(k1(4,j)+2*k2(4,j)+2*k3(4,j)+k4(4,j));
    phi2(j+1)=phi2(j)+1/6*dx*(k1(5,j)+2*k2(5,j)+2*k3(5,j)+k4(5,j));
    phi3(j+1)=phi3(j)+1/6*dx*(k1(6,j)+2*k2(6,j)+2*k3(6,j)+k4(6,j));
    theta(j+1)=2*phi1(j+1)-phi2(j+1)-dk*x(j+1);
    omega(j+1)=phi1(j+1)+phi2(j+1)-phi3(j+1)-deltak*x(j+1);
end
plot(x/epsilon,alpha1)
hold on
plot(x/epsilon,abs(alpha2),'r')
hold on
plot(x/epsilon,abs(alpha3),'g')
xlabel('Distance (m)'),ylabel('Amplitude (m)'),title('Amplitudes of First Three Harmonics
by Splitting into Amplitude and Phase')
legend('1st Mode','2nd Mode','3rd Mode')
```

APPENDIX C: MATLAB CODE FOR SOLVING THE EVOLUTION EQUATIONS BY SPLITTING THE COMPLEX FUNCTION INTO REAL AND IMAGINARY PARTS

```
% RK4 real equation a(X) solver for the evolution equations
% using a(X)=p(X)+iq(X)
clear,clc
h=0.4;
T=2.5;
g=9.81;
H=0.084;
a1=H/2;
a2=1e-10;
a3=1e-10;
epsilon=a1/h;
% epsilon=0.45;
dx=0.05*epsilon;
x=0:dx:30*epsilon;
n=length(x);
alpha1=zeros(size(x));
alpha2=zeros(size(x));
alpha3=zeros(size(x));
phi1=zeros(size(x));
phi2=zeros(size(x));
phi3=zeros(size(x));
alpha1(1)=a1;
alpha2(1)=a2;
alpha3(1)=a3;
alpha1tmp=zeros(size(x));
alpha2tmp=zeros(size(x));
alpha3tmp=zeros(size(x));
phi1tmp=zeros(size(x));
phi2tmp=zeros(size(x));
phi3tmp=zeros(size(x));
w0=2*pi/T;
w=[w0,2*w0,3*w0];
b=1/15;
k=sqrt(((1/3+b)*h^2*w.^2-g*h+sqrt(((1/3+b)*h^2*w.^2-
g*h).^2+4*b*g*w.^2*h^3))/(2*b*g*h^3)); %when b=1/15 from eqn.(5.122) on book
p.524
%set S,P and Q
S=2*g.*w.*(1-h*w.^2/g*(1/3+b)+3*b*h^2*k.^2/2);
Q1=g*(k(2)-k(1))^2*(w(1)/k(1)+w(2)/k(2))/h+w(1)*w(2)*(1/k(1)-1/k(2))*(w(2)-
w(1))/h^2;
P1=g*(k(3)-k(2))^2*(w(3)/k(3)+w(2)/k(2))/h+w(3)*w(2)*(1/k(2)-1/k(3))*(w(3)-
w(2))/h^2;
Q2=4*g*w(1)*k(1)/h+2*(w(1))^3/k(1)/h^2;
```

```
P2=g*(k(3)-k(1))^2*(w(3)/k(3)+w(1)/k(1))/h+w(3)*w(1)*(1/k(1)-1/k(3))*(w(3)-
w(1))/h^2;
P3=g*(k(1)+k(2))^2*(w(1)/k(1)+w(2)/k(2))/h+w(1)*w(2)*(1/k(2)+1/k(1))*(w(1)+w(2))/
h^2;
T1=Q1./S(1);
T2=Q2./S(2);
S1=P1./S(1);
S2=P2./S(2);
S3=P3./S(3);
dk=(k(2)-2*k(1))/epsilon;
deltak=(k(3)-k(2)-k(1))/epsilon;
theta=2*phi1-phi2-dk*x;
omega=phi1+phi2-phi3-deltak*x;
thetatmp=zeros(size(x));
omegatmp=zeros(size(x));

for j=1:n-1
   %     set k1
   k1(1,j)=-(T1*alpha1(j)*alpha2(j)*sin(theta(j))+S1*alpha2(j)*alpha3(j)*sin(omega(j)));
   k1(2,j)=T2*alpha1(j)^2*sin(theta(j))-S2*alpha1(j)*alpha3(j)*sin(omega(j));
   k1(3,j)=S3*alpha1(j)*alpha2(j)*sin(omega(j));
   k1(4,j)=-(T1*alpha2(j)*cos(theta(j))+S1*alpha2(j)*alpha3(j)/alpha1(j)*cos(omega(j)));
   k1(5,j)=-T2*alpha1(j)^2/alpha2(j)*cos(theta(j))-
S2*alpha1(j)*alpha3(j)/alpha2(j)*cos(omega(j));
   k1(6,j)=-S3*alpha1(j)*alpha2(j)/alpha3(j)*cos(omega(j));
   alpha1tmp(j)=alpha1(j)+1/2*dx*k1(1,j);
   alpha2tmp(j)=alpha2(j)+1/2*dx*k1(2,j);
   alpha3tmp(j)=alpha3(j)+1/2*dx*k1(3,j);
   phi1tmp(j)=phi1(j)+1/2*dx*k1(4,j);
   phi2tmp(j)=phi2(j)+1/2*dx*k1(5,j);
   phi3tmp(j)=phi3(j)+1/2*dx*k1(6,j);
   thetatmp(j)=2*phi1tmp(j)-phi2tmp(j)-dk*(x(j)+dx/2);
   omegatmp(j)=phi1tmp(j)+phi2tmp(j)-phi3tmp(j)-deltak*(x(j)+dx/2);
   %     set k2
   k2(1,j)=-
(T1*alpha1tmp(j)*alpha2tmp(j)*sin(thetatmp(j))+S1*alpha2tmp(j)*alpha3tmp(j)*sin(om
egatmp(j)));
   k2(2,j)=T2*alpha1tmp(j)^2*sin(thetatmp(j))-
S2*alpha1tmp(j)*alpha3tmp(j)*sin(omegatmp(j));
   k2(3,j)=S3*alpha1tmp(j)*alpha2tmp(j)*sin(omegatmp(j));
   k2(4,j)=-
(T1*alpha2tmp(j)*cos(thetatmp(j))+S1*alpha2tmp(j)*alpha3tmp(j)/alpha1tmp(j)*cos(om
egatmp(j)));
   k2(5,j)=-T2*alpha1tmp(j)^2/alpha2tmp(j)*cos(thetatmp(j))-
S2*alpha1tmp(j)*alpha3tmp(j)/alpha2tmp(j)*cos(omegatmp(j));
   k2(6,j)=-S3*alpha1tmp(j)*alpha2tmp(j)/alpha3tmp(j)*cos(omegatmp(j));
```

```
   alpha1tmp(j)=alpha1(j)+1/2*dx*k2(1,j);
   alpha2tmp(j)=alpha2(j)+1/2*dx*k2(2,j);
   alpha3tmp(j)=alpha3(j)+1/2*dx*k2(3,j);
   phi1tmp(j)=phi1(j)+1/2*dx*k2(4,j);
   phi2tmp(j)=phi2(j)+1/2*dx*k2(5,j);
   phi3tmp(j)=phi3(j)+1/2*dx*k2(6,j);
   thetatmp(j)=2*phi1tmp(j)-phi2tmp(j)-dk*(x(j)+dx/2);
   omegatmp(j)=phi1tmp(j)+phi2tmp(j)-phi3tmp(j)-deltak*(x(j)+dx/2);
   %     set k3
   k3(1,j)=-
(T1*alpha1tmp(j)*alpha2tmp(j)*sin(thetatmp(j))+S1*alpha2tmp(j)*alpha3tmp(j)*sin(om
egatmp(j)));
   k3(2,j)=T2*alpha1tmp(j)^2*sin(thetatmp(j))-
S2*alpha1tmp(j)*alpha3tmp(j)*sin(omegatmp(j));
   k3(3,j)=S3*alpha1tmp(j)*alpha2tmp(j)*sin(omegatmp(j));
   k3(4,j)=-
(T1*alpha2tmp(j)*cos(thetatmp(j))+S1*alpha2tmp(j)*alpha3tmp(j)/alpha1tmp(j)*cos(om
egatmp(j)));
   k3(5,j)=-T2*alpha1tmp(j)^2/alpha2tmp(j)*cos(thetatmp(j))-
S2*alpha1tmp(j)*alpha3tmp(j)/alpha2tmp(j)*cos(omegatmp(j));
   k3(6,j)=-S3*alpha1tmp(j)*alpha2tmp(j)/alpha3tmp(j)*cos(omegatmp(j));
   alpha1tmp(j)=alpha1(j)+dx*k3(1,j);
   alpha2tmp(j)=alpha2(j)+dx*k3(2,j);
   alpha3tmp(j)=alpha3(j)+dx*k3(3,j);
   phi1tmp(j)=phi1(j)+dx*k3(4,j);
   phi2tmp(j)=phi2(j)+dx*k3(5,j);
   phi3tmp(j)=phi3(j)+dx*k3(6,j);
   thetatmp(j)=2*phi1tmp(j)-phi2tmp(j)-dk*(x(j)+dx);
   omegatmp(j)=phi1tmp(j)+phi2tmp(j)-phi3tmp(j)-deltak*(x(j)+dx);
   %     set k4
   k4(1,j)=-
(T1*alpha1tmp(j)*alpha2tmp(j)*sin(thetatmp(j))+S1*alpha2tmp(j)*alpha3tmp(j)*sin(om
egatmp(j)));
   k4(2,j)=T2*alpha1tmp(j)^2*sin(thetatmp(j))-
S2*alpha1tmp(j)*alpha3tmp(j)*sin(omegatmp(j));
   k4(3,j)=S3*alpha1tmp(j)*alpha2tmp(j)*sin(omegatmp(j));
   k4(4,j)=-
(T1*alpha2tmp(j)*cos(thetatmp(j))+S1*alpha2tmp(j)*alpha3tmp(j)/alpha1tmp(j)*cos(om
egatmp(j)));
   k4(5,j)=-T2*alpha1tmp(j)^2/alpha2tmp(j)*cos(thetatmp(j))-
S2*alpha1tmp(j)*alpha3tmp(j)/alpha2tmp(j)*cos(omegatmp(j));
   k4(6,j)=-S3*alpha1tmp(j)*alpha2tmp(j)/alpha3tmp(j)*cos(omegatmp(j));
   %     calculate a
   alpha1(j+1)=alpha1(j)+1/6*dx*(k1(1,j)+2*k2(1,j)+2*k3(1,j)+k4(1,j));
   alpha2(j+1)=alpha2(j)+1/6*dx*(k1(2,j)+2*k2(2,j)+2*k3(2,j)+k4(2,j));
   alpha3(j+1)=alpha3(j)+1/6*dx*(k1(3,j)+2*k2(3,j)+2*k3(3,j)+k4(3,j));
```

```
    phi1(j+1)=phi1(j)+1/6*dx*(k1(4,j)+2*k2(4,j)+2*k3(4,j)+k4(4,j));
    phi2(j+1)=phi2(j)+1/6*dx*(k1(5,j)+2*k2(5,j)+2*k3(5,j)+k4(5,j));
    phi3(j+1)=phi3(j)+1/6*dx*(k1(6,j)+2*k2(6,j)+2*k3(6,j)+k4(6,j));
    theta(j+1)=2*phi1(j+1)-phi2(j+1)-dk*x(j+1);
    omega(j+1)=phi1(j+1)+phi2(j+1)-phi3(j+1)-deltak*x(j+1);
end
plot(x/epsilon,alpha1)
hold on
plot(x/epsilon,abs(alpha2),'r')
hold on
plot(x/epsilon,abs(alpha3),'g')
xlabel('Distance (m)'),ylabel('Amplitude (m)'),title('Amplitudes of First Three Harmonics
by Splitting into Amplitude and Phase')
legend('1st Mode','2nd Mode','3rd Mode')
```

VITA

Qian Zhang was born on July 4, 1983, in Harbin, Hei Longjiang, China. She received her Bachelor of Science in Automation from Harbin Engineering University, China in May, 2006 and a Master of Science in Control & Mechatronics Engineering from Harbin Institute of Technology, China, in May, 2008. She entered the Department of Civil and Environmental Engineering (Engineering Science) at Louisiana State University in fall 2008 and has been working on numerical modeling of water waves and coastal hydrodynamics. She expects to earn a Master of Science in Engineering Science in June, 2011, and continue to pursue a doctorate.